AB Statens Anläggningsprovning

Alströmergatan 12 · Box 49306 · 100 28 STOCKHOLM · Tel. 08–54 10 20

A DYNAMIC ANALYSIS OF CRACK PROPAGATION AND ARREST OF PRESSURIZED THERMAL SHOCK EXPERIMENTS (PTSE)

BJÖRN BRICKSTAD, SA
FRED NILSSON, SKI

SA/FoU-RAPPORT 85/01
SKI-projekt nr B114/84

A DYNAMIC ANALYSIS OF CRACK PROPAGATION AND ARREST OF PRESSURIZED THERMAL SHOCK EXPERIMENTS (PTSE).

Björn Brickstad
The Swedish Plant Inspectorate
Box 49306
S-100 28 STOCKHOLM
SWEDEN

Fred Nilsson
Swedish Nuclear Power Inspectorate
Box 27106
S-102 52 STOCKHOLM
Sweden

Abstract

The PTS-experiments performed at ORNL are dynamically analysed by aid of a two-dimensional FEM-code with capability of simulating rapid crack growth. It is found that both a quasistatic and a dynamic treatment agree well with the experimentally obtained crack arrest lengths.

Introduction

The origin to this analysis stems from the International Conference on Dynamic Fracture Mechanics, which was held in San Antonio, Texas, 7-9 November 1984. A topic at that conference which was the object of many discussions, was the application of dynamic fracture mechanics to the pressurized thermal shock (PTS) problem. Brickstad and Nilsson [1] presented a dynamic analysis of crack arrest in a nuclear pressure vessel subjected to postulated PTS-transients. It was found that for the analysed cases, a quasistatic treatment was slightly conservative.

Recently, large scale PTS-experiments (Bryan et al [2]) have been performed at ORNL and it was suggested at the conference that the dynamic analysis should be extended to these experiments in order to investigate the role of dynamic effects also under real experimental situations.

In the following analysis, the basic assumptions and numerical treatment are identical to those stated in [1], and the reader is referred to that paper for a more detailed description of the underlying procedure.

Description of the studied PTS-experiments.

The PTSE-vessel geometry consisted of a cylindrical pressure vessel with an inside radius of 343.0 mm and a thickness of 147.6 mm. The material properties were those of SA508, class 2 and are given in table 1. The vessel was given a long axial crack from the outside and in order to initiate crack growth the cooling was made on the cracked side of the vessel. The temperature distributions for the two experiments PTSE-1B and 1C were measured by aid of thermocouples and are shown in fig. 1 (Bass [3]). Also indicated in fig. 1 are the initial crack length a_o, the crack arrest length a_f and the internal pressure p_o at initiation of crack growth.

The fracture properties for the crack arrest toughness K_{Ia} and the crack propagation toughness K_{pc}, are almost identical to the relations used in ref. [1]. The dependence on temperature T and crack velocity $\dot{a}$ are assumed as

$$K_{Ia}(T) = 35.0 + 4.0177 \cdot \exp(0.02408 \cdot T) \text{ MPa}\sqrt{\text{m}} \tag{1}$$

$$K_{pc}(\dot{a}, T) = K_{Ia} + A \cdot \dot{a}^2 \tag{2}$$

$$A = \begin{cases} (32.97 + 1.625(T-RT_{NDT})) \cdot 10^{-5} \text{ MPam}^{-3/2}\text{ s}^2 & T-RT_{NDT} > -13.9^oC \\ (121.71+1.2962\ (T-RT_{NDT})) \cdot 10^{-6} \text{ MPam}^{-3/2}\text{ s}^2 & T-RT_{NDT} \leq -13.9^oC \end{cases} \tag{3}$$

However K_{Ia} is not bounded by any upper shelf-level, as was done in [1].

Method of analysis

The two-dimensional FEM-mesh modelling half a ring of the PTSE-vessel is shown in fig. 2. It consists of 400 3- and 4-node elements giving a minimum of 804 degrees of freedom. The smallest element size at the crack plane is 4 x 5 mm. A calibration of the FEM-grid was made by comparing the static stress intensity factor K_I^s, calculated by an energy method from the mesh in fig. 2 and taken from the solution given by Delale and Erdogan [4] for an external axial crack in a hollow cylinder under internal pressure. The numerical solution slightly underestimates the solution in [4], of the order of five per cent for the crack length intervals obtained in the PTS-experiments.

The numerical procedure for predicting a crack arrest event is identical to [1]. In short, the initial static state is first determined for the particular loading at the considered initial crack length. With this as input into the dynamic analysis, the crack growth is determined such that the dynamic stress intensity factor K_I^d equals the crack propagation toughness K_{Ipc}. A crack arrest is then predicted if the solution gives $\dot{a} = 0$ for a certain crack length, corresponding to $K_I^d = K_{Ia}$. For comparison, the static stress intensity factor K_I^s, neglecting inertia effects, is also calculated.

Results and discussion

In figs. 3-4, for the two PTS-experiments, the different stress intensity factors K_I^s, K_I^d and the predicted crack velocity $\dot{a}$ are shown as functions of the crack length as mesured from the outside wall of the cylinder. Also shown is the crack arrest toughness K_{Ia} for which a sharp increase is seen due to the steep temperature gradients. A quasistatic arrest is predicted at the intersection between K_I^s and K_{Ia}. The symbols in the figures are referring to the midside of the finite elements along the crack plane and a dynamically predicted crack arrest, as indicated by an arrow in the figures, is attributed to a position of a nodal point of the FEM-grid.

The results in figs. 3-4 are reflecting the same principal behaviour as in [1]. During the short time interval when the crack propagates, K_I^d is slightly smaller than K_I^s. At crack arrest both the quasistatic and dynamic treatments give accurate predictions of the experimental arrest length. In table 2 the different crack arrest lengths are compared with the actual experimental results. They are essentially coinciding, within the computational accuracy, and it appears that theory and experiments are in good agreement. However, one may argue that in these experiments, due to the steep temperature gradients, $K_{Ia}(T)$

increases so rapidly that a crack arrest is sure to be predicted, regardless of method, within a short distance from the experimental values. This means that for a more discriminative test regarding the accuracy of quasi-static compared to dynamic predictions of crack arrest, a less steep temperature profile should be used.

It is also interesting to note that for the PTSE-1C event, since K_I^s is a strictly increasing function of crack length, a crack arrest would never be predicted if the commonly assumed upper shelf-level of 220 MPa$\sqrt{m}$ had been used for K_{Ia}. This illustrates our limited knowledge of the fracture properties of the material at high temperatures.

As in [1], a sensitivity study was performed regarding the influence upon the results from the velocity--dependence of K_{Ic}. This time, the PTSE-1C event was reanalysed assuming $K_{Ic}(\dot{a}, T) = K_{Ia}(T)$, i.e. no velocity-depandence at all. As in [1], the different $K_{Ic}(\dot{a})$ -relations resulted in identical crack arrest length predictions, the difference here being that a much higher crack velocity was predicted during the propagation phase. However, the convergence of the numerical procedure to predict the crack growth appearred to be slower when the velocity-dependence of K_{Ic} was removed. This is quite natural since the velocity--dependence of K_I^d, within each crack growth interval, is fairly weak.

It may thus be concluded that in PTS-problems with relatively steep temperature gradients, if the primary object is to predict the crack arrest length, it is more important to have accurate information about the temperature-dependence of $K_{Ic}(\dot{a}, T)$ than the velocity--dependence. This conclusion is supported by Jung and Kanninen [5] in their analysis of thermal shock experiments. They found that the crack arrest length predictions were sensitive to the temperature-dependence of K_{Ia}. Furthermore, it seems as if these crack arrest predictions can be made with sufficient accuracy for engineering purposes with quasi-static methods, at least for limited amount of crack growth. It should be reminded, however, if the object is to determine K_{Ia} in experiments, it is in general important to have accurate information about the crack velocity, to use it in a dynamic analysis to determine K_{Ia}. Quasi-statically determined K_{Ia} -values have been shown to be history--dependent.

Acknowledgement

This work was sponsored by the Swedish Nuclear Power Inspectorate and this support is gratefully acknowledged. We also want to thank Dr. C.E. Pugh and Dr. B.R. Bass for helpful information about the PTS-experiments at ORNL.

References

[1] B. Brickstad and F. Nilsson, "Dynamic analysis of crack growth and arrest in a pressure vessel subjected to thermal and pressure loading", Proc. from Int. Conf. on Dynamic Fracture Mechanics, San Antonio, Texas, Nov. 1984.

[2] R.H. Bryan, B.R. Bass, S.E. Bolt, J.W. Bryson, J.G. Merkle, G.C. Robinson and G.D. Whitman, "Quick-Look report on the first pressurized thermal shock test PTSE-1", Oak Ridge National Laboratory ORNL/PTSE-1, 1984.

[3] B.R. Bass. Private communication.

[4] F. Delale and F. Erdogan, "Stress intensity factors in a hollow cylinder containing a radial crack", Int. J. Fract., 20, 251-265, 1982.

[5] J. Jung and M.F. Kanninen, "An analysis of dynamic crack propagation and arrest in a nuclear pressure vessel under thermal shock conditions", J. of Pressure Vessel Tech., 105, 111-116, 1983.

Figure captions

Fig. 1 Temperature gradients for PTS-experiments 1B and 1C. X is measured from the inside wall.

Fig. 2 Finite element model of the PTS-cylinder.

Fig. 3 K_{Ia}, K_I^s, K_I^d and å as functions of crack length a for PTSE-1B.

Fig. 4 K_{Ia}, K_I^s, K_I^d and å as functions of crack length a for PTSE-1C.

Table 1. Material properties of the SA508-steel used for the PTS-experiments.

Young's modulus	$E = 2.023 \times 10^5$ MPa
Poisson's ratio	$\nu = 0.3$
Mass density	$\rho = 7850$ kg/m^3
Thermal expansion coefficient	$\alpha = 14.4 \times 10^{-6}$ $^oC^{-1}$
Nil-ductility temperature	$RT_{NDT} = 91.3$ ^oC

Table 2. Comparison of quasi-static and dynamic crack arrest lengths with ORNL experimental results. All measured in mm.

Event	Quasi-static	Dynamic	Experimental
PTSE-1B	23.0	24.0	24.4
PTSE-1C	39.0	40.0	41.0

Fig. 1

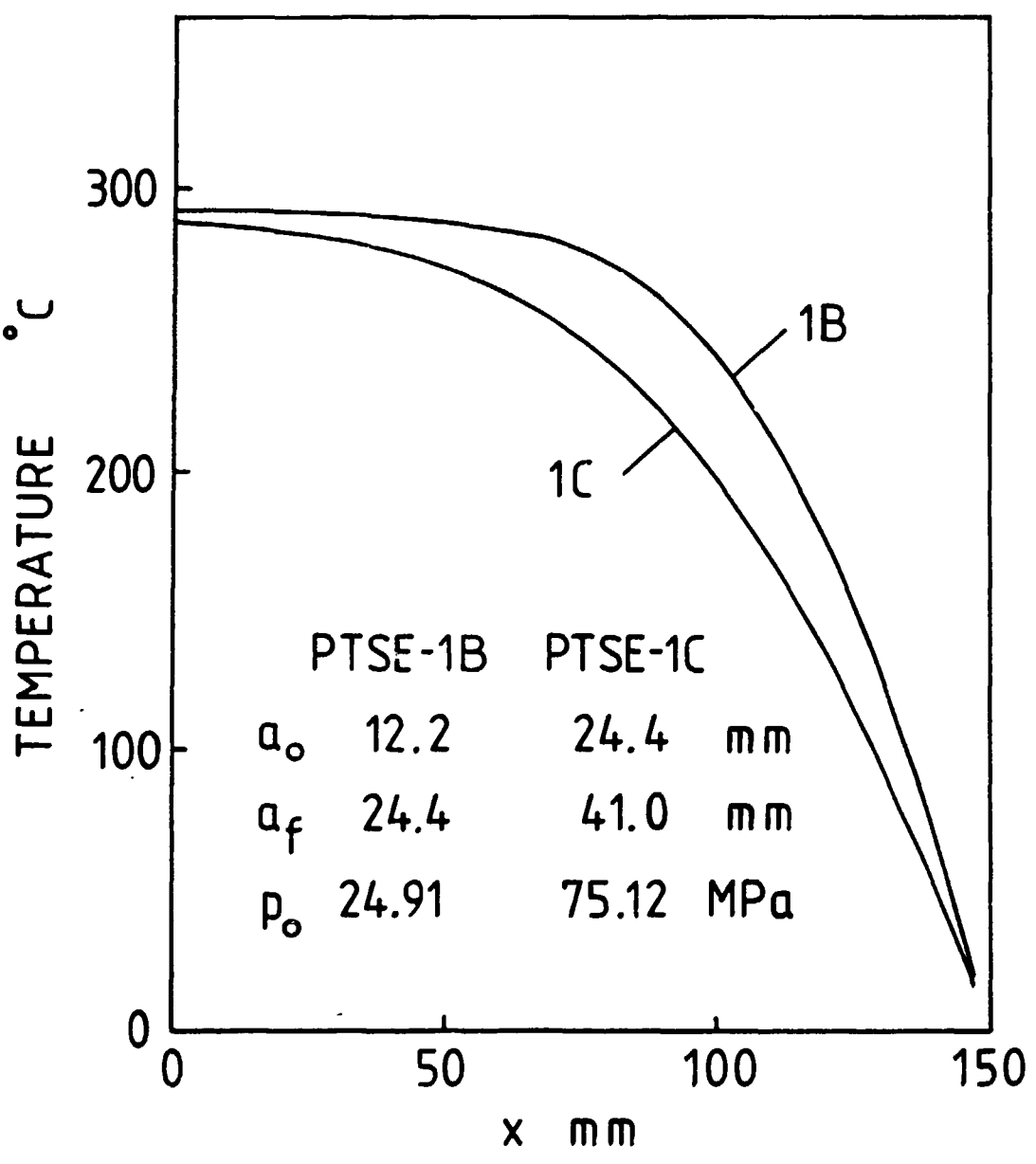
TEMPERATURE °C
300
200
100
0
0
50
100
150
x mm
1B
1C
PTSE-1B PTSE-1C
a_o 12.2 24.4 mm
a_f 24.4 41.0 mm
p_o 24.91 75.12 MPa

Fig. 2

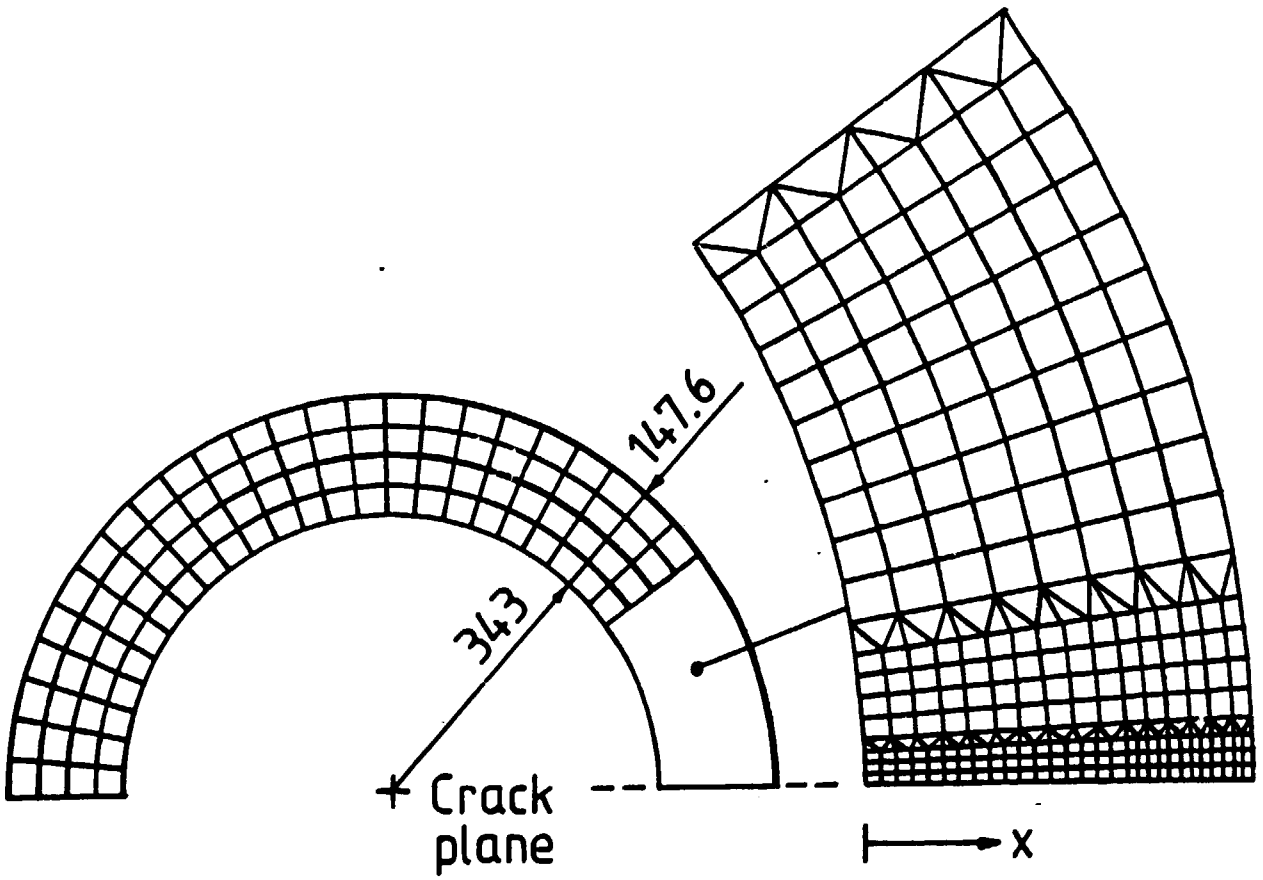

Fig. 3

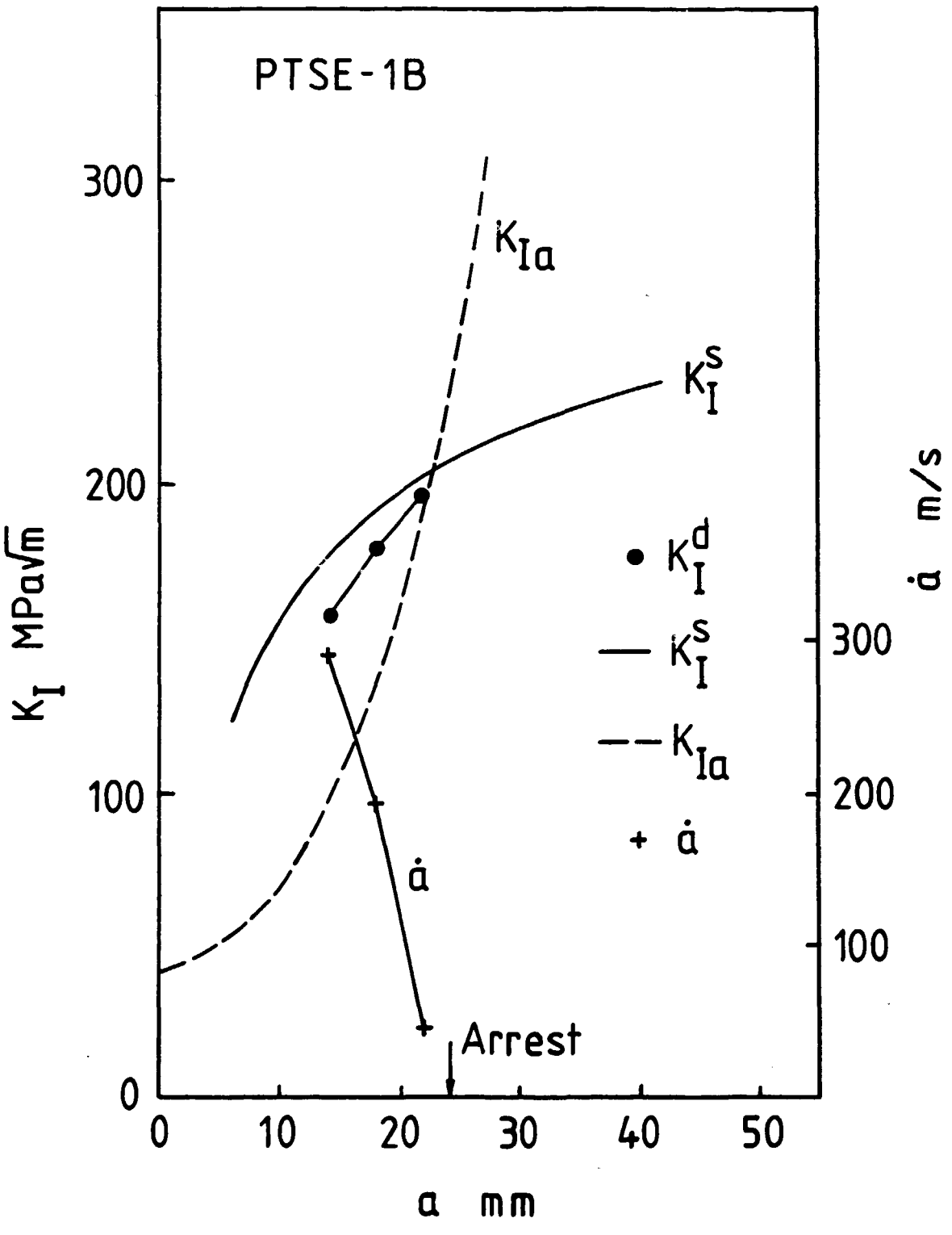
PTSE-1B
300
200
100
0
K_{Ia}
K_I^s
K_I^d
K_I^s
K_{Ia}
$\dot{a}$
$\dot{a}$
Arrest
K_I MPa$\sqrt{m}$
$\dot{a}$ m/s
300
200
100
0
10
20
30
40
50
a mm

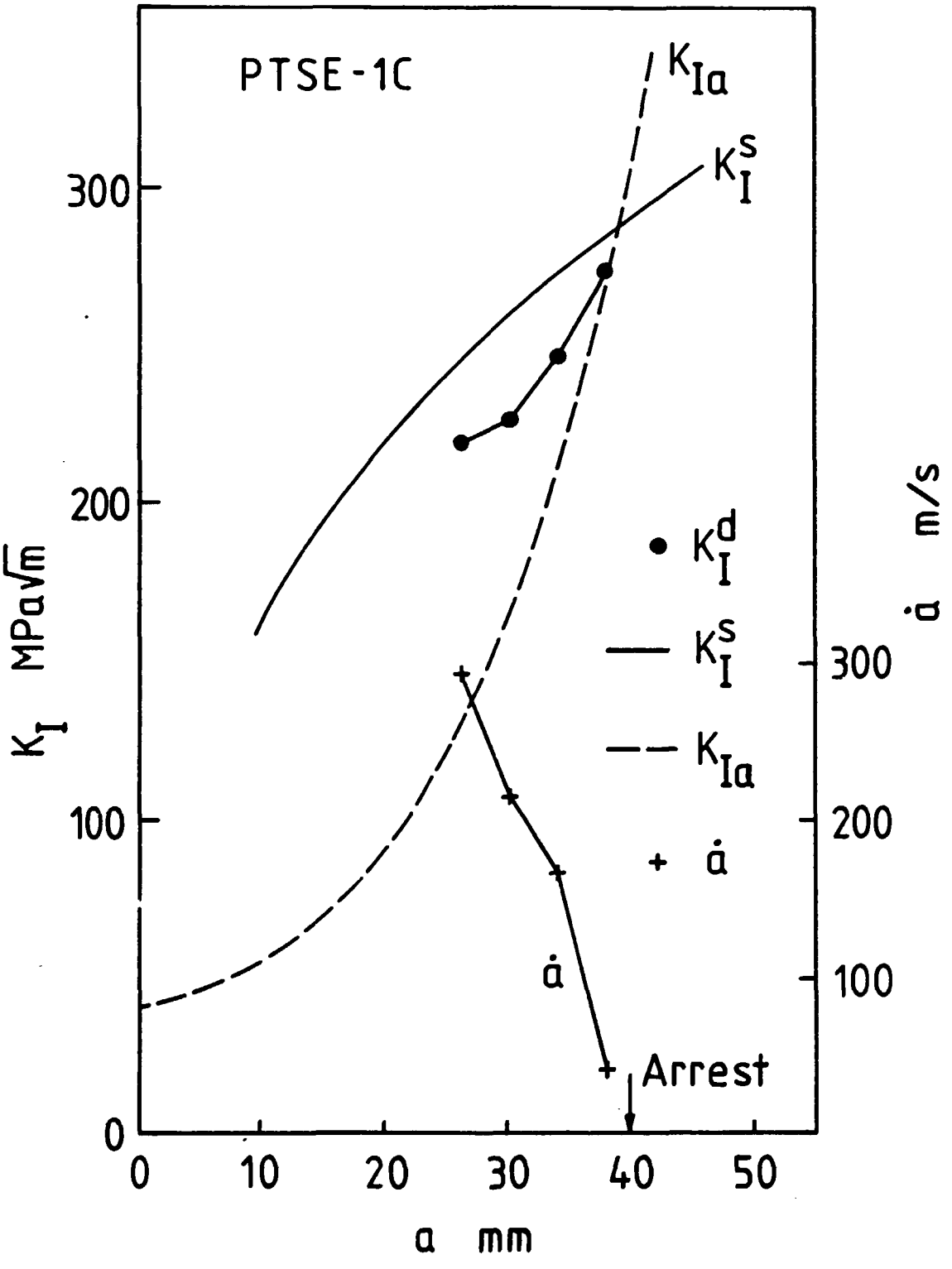
PTSE-1C
K_{Ia}
K_I^s
300
200
100
0
K_I MPa$\sqrt{m}$
K_I^d
K_I^s
K_{Ia}
$\dot{a}$
$\dot{a}$
Arrest
300
200
100
$\dot{a}$ m/s
0
10
20
30
40
50
a mm